

# Using Perturbative Least Action to Reconstruct the Local Group

David M. Goldberg

Yale University, Astronomy Dept., New Haven, CT, 06520-8101

Princeton University Observatory, Princeton, NJ 08544-1001

## ABSTRACT

In this paper, we apply the Perturbative Least Action Method to model the Local Group of galaxies for various Cosmological models. We show that though the galaxy masses are theoretically good discriminators of  $\Omega_M$  given some observed MW and M31 separation and radial velocity, current estimates of the masses are insufficient to make any cosmological claims. We then discuss additional complications to expand this analysis.

## 1. Introduction

The dynamics of the Local Group of galaxies (LG; see Van den Bergh 1999; 2000; Mateo 1998, and references therein for recent reviews) can potentially provide a wealth of information both about the component galaxies and the underlying cosmological parameters (Governato et al. 1997).

Kahn & Woltjer (1959; see Peebles 1993 for a discussion) are the first to suggest that the radial velocity of M31 toward the Galaxy could be used as a means of estimating the combined mass of the Local Group system. Since the separation and radial velocity of the two galaxies were known, they reasoned that the Local Group could be treated as a simple two-body problem.

The observed separation of the two galaxies is well constrained. Holland (1998) estimates the separation to be 745 kpc, while Mateo (1998) in his excellent review of the dwarf galaxies in the Local group gives a distance of 770 kpc. A middle value of 760 kpc is given by van den Bergh (1999; 2000), a value we will adopt throughout the remaining discussion.

The cosmological parameters  $H_0$ ,  $\Omega_M$  and  $\Omega_\Lambda$  uniquely give an age of the universe. Thus the expected radial velocity in this simplified model is a function of cosmology, observed separation, and total mass of the system, as would be expected. This observed radial velocity, after subtracting the velocity of the Sun around the center of the Milky

Way is approximately -119 km/s (Binney & Tremaine, 1987 using solar velocity estimates of Lynden-Bell et al., 1983). We show the mass-velocity relation for two-body Local Group models in Figure 1, demonstrating that for reasonable cosmologies, this method implies that the integrated Local Group mass must be at least  $4 \times 10^{12} M_{\odot}$ , and perhaps as high as  $6 \times 10^{12} M_{\odot}$ .

These estimated masses are on the high side of observations. van den Bergh (1999; 2000) gives an integrated mass of the Local Group of  $(2.3 \pm 0.6) \times 10^{12} M_{\odot}$ , based on dispersion of component galaxy radial velocity measurements.

Masses for the individual components have varied somewhat in recent years. Zaritsky (1999) estimates the mass of the Galaxy as  $8.6 \times 10^{11} M_{\odot}$  based on a combination of globular cluster observations (out to  $\sim 50$  kpc), and dwarf spheroidal observations (out to  $\sim 250$  kpc). Wilkinson & Evans(1999) primarily analyze recent dwarf spheroidal measurements, and use them to compute a detailed density profile of the Galaxy, yielding a much larger estimate of  $1.9 \times 10^{12} M_{\odot}$ , albeit with very large error bars.

Mass estimates for M31 are somewhat more tightly clustered, with typical estimates of  $2.3 \times 10^{12} M_{\odot}$  estimated for the entire subgroup (Courteau & van den Bergh 1999), and  $1.2 \times 10^{12} M_{\odot}$ , again based on radial velocity measurements of dwarf spheroidals (Evans & Wilkinson 2000).

A somewhat better treatment of the dynamics of the Galaxy-M31 system can be had by treating the two galaxies explicitly as particles in the cosmic flow. This is the approach taken by Peebles (1989) in describing a cosmological least action approach to solving particle trajectories.

Treating M31, the Galaxy, six Local Group Dwarf galaxies, and a number of nearby groups as point sources, he is able to calculate orbits using a Least Action approach. By varying cosmology, and comparing the resulting distances and masses of the galaxies to their observed values, he finds high Galaxy masses ( $M_{LG} \simeq 5 - 6 \times 10^{12} M_{\odot}$ ) for high  $\Omega_M$  models, but good agreement with the local distance scale. Low  $\Omega_M$  models, on the other hand, yielded lower mass estimates ( $M_{LG} = 3.2 - 4.4 \times 10^{12} M_{\odot}$ ), and correspondingly worse distance estimates between M31 and the Galaxy, but better distance estimates to nearby groups. Since different cosmologies provide better fits to different observables, he makes no definitive conclusions about the true, underlying cosmology.

Shaya, Peebles, and Tully (1995) extend this technique considerably beyond the Local Group, to model galaxy orbits out to 3000 km/s. From this survey, they estimate a value of  $\Omega_M = 0.17 \pm 0.10$ . Dunn & Laflamme (1993) find a similar result, also suggesting a low  $\Omega_M$ . Schmoldt & Saha (1998) use the observed velocity, rather than the distance, of M31

as a constraint, and measure a Local Group mass of  $4 - 8 \times 10^{12} h^{-1} M_{\odot}$ , again, producing a much larger mass than most observational evidence would suggest.

Branchini & Carlberg (1995) object to this approach, however. They point out that in actual fact, galaxies did not exist as point masses at any point in their history, and were, rather, collapsing halos which overlap one another even today. To test whether this would affect corresponding mass estimates, they ran a number of N-body simulations and compared the true masses and trajectories of “galaxies” in their simulations to the masses and trajectories which could be imputed using a Least Action approach. They find that the point mass assumption is not necessarily a valid one, and that it leads to an underestimated value of  $\Omega_M$ . They suggest that even  $\Omega_M = 1$  is consistent with Local Group dynamics.

Goldberg & Spergel (2000, GS; Goldberg 2000) revisit the problem of reconstructing orbits by introducing Perturbative Least Action (PLA). PLA gets around the objections raised by Branchini and Carlberg by treating galaxies not as point sources, but rather as part of a continuous fluid which collapse over the course of a simulation. Furthermore, since the orbits are constrained to grow linearly from a uniform field at early times, the Zel’dovich (1970) approximation necessarily holds.

Given PLA’s ability to model the history of highly overdense systems, the Local Group seems a natural target of investigation. In particular one may use radial velocity and distance measurements to estimate the masses of M31 and the Galaxy, and to make predictions about cosmology. In § 2, we review the Perturbative Least Action method, and describe its applications. In § 3, we model a simplified Local Group in several cosmologies, in essence duplicating the Kahn & Woltjer (1959) analysis for the case of known final masses and with the assumption that galaxies form from the collapse of the initially smooth density field. We will show that even this toy model may provide insight into the underlying cosmology. Finally, in § 4, we discuss some potentially useful avenues of future study.

## 2. Perturbative Least Action

Before describing the Local Group simulations, it might be productive to briefly review the PLA method. Interested readers will find a more complete discussion in GS and Goldberg (2000).

The aim of PLA and methods like it is to reconstruct the initial conditions of observed structure in the universe. In essence, this means that we wish to run an N-body calculation “backwards in time.” In order to accomplish this, we will make a number of simplifying assumptions. First, we treat the energy density of the universe as consisting solely as Cold

Dark Matter (CDM) and hence the only force acting on the field will be gravity. Secondly, the matter is treated as a distribution of small point masses, which, when smoothed, reproduce an observed density field.

In order to provide a context, let us imagine a particle field at  $a = 0$  (where  $a$  is the normalized expansion parameter of the universe) which is uniformly distributed, and which has zero comoving velocity. We will label the unperturbed particle positions,  $\{\mathbf{q}_i\}$  (where here and throughout, all particle positions are assumed to be given in comoving coordinates). At a slightly later time,  $t_i$ , the particles are offset slightly,  $\mathbf{p}_i(t_i) = \mathbf{p}(\mathbf{q}_i, t_i)$ , from their gridpoints, such that:

$$\mathbf{x}_i(t_i) = \mathbf{q}_i + \mathbf{p}_i(t_i) , \quad (1)$$

Linear perturbation theory can be used to demonstrate that small perturbations grow monotonically with time. In §2.2.1, we showed this yields the relation:

$$\mathbf{p}_i(t) = \frac{D(t)}{D(t_i)} \mathbf{p}_i(t_i) , \quad (2)$$

where  $D(t)$  is the cosmologically determined linear growth factor, normalized to unity at the present. The combination of equations (1) and (2) are known as the Zel’dovich (1970) approximation, and describes the growth of structure well so long as perturbations are small.

As perturbations grow to the point when particle trajectories cross one another, the orbits become more complex. This is essentially why N-body simulations are needed in the first place; the trajectories of particles are strongly coupled, and no analytic solutions exist for orbits of more than two interacting particles.

In general, N-body simulations are run forward in time. However, Peebles (1989) pointed out that if we specify the initial and final position of a particle rather than the initial position and velocity, the trajectory may be solved by finding the path which minimizes the action (the time integral of the Lagrangian):

$$S \equiv \sum_i \int_0^{t_0} dt \mathcal{L}_i = \sum_i \int dt \left( \frac{a^2 \dot{\mathbf{x}}_i^2}{2} - \frac{\phi_i}{2} \right) , \quad (3)$$

where  $\phi_i$  is the potential on particle  $i$ .

While Peebles (1989; 1993; 1994) and others (Shaya, Peebles, & Tully 1995; Schmoldt & Saha 1998) have historically calculated the particle potentials ( $\phi_i$ ) by direct summation, this is impractical as the number of particles gets large. We get around this by using a

Particle Mesh (PM) Poisson solver (Hockney & Eastwood 1981), which requires computing time of order  $N \log_2 N$ , rather than  $N^2$ . Nusser and Branchini (1999) use a similar approach in their Least Action technique by utilizing a tree code for their Poisson solver.

The PLA method involves running a randomly realized N-body simulation, and storing the output trajectories which we will call  $\mathbf{x}_i^{(0)}(t)$ . Since the “unperturbed” orbit is known to satisfy the equations of motion at all times, we may express the “perturbed” trajectory as:

$$\mathbf{x}_i(t) = \mathbf{x}_i^{(0)}(t) + \mathbf{x}_i^{(1)}(t) . \quad (4)$$

These trajectories are then subject to the constraints  $\mathbf{x}_i(0) = \mathbf{q}_i$  and  $\mathbf{x}_i(t_0) = \mathbf{x}_i^F$ . GS and Goldberg (2000) discuss how one generates the final the set of final constraints,  $\mathbf{x}_i^F$  for a given set of observations.

Once we’ve computed the boundary constraints on each particle, it remains for the orbit of each particle to be parameterized so that we can find the minimal action orbits. We express the trajectory of each particle as:

$$\mathbf{x}_i(t) = \mathbf{x}_i^{(0)}(t) + D(t)\mathbf{x}_i^{(1)F} + \sum_{n=1}^{n_{max}} \mathbf{C}_{i,n} f_n(t) , \quad (5)$$

where  $\mathbf{x}_i^{(1)F} \equiv \mathbf{x}_i^F - \mathbf{x}_i^{(1)}(t_0)$ ,  $\mathbf{C}_{i,n}$  are a set of coefficients, and  $f_n(t)$ , are a set of basis functions. We have found it useful to use the form:

$$f_n(t) = \sum_{m=n}^{n_{max}} b_{mn} D(t) [1 - D(t)^m] . \quad (6)$$

As a result, only the first basis function varies as slowly as linearly at early times, and no decaying modes can be expressed. Thus, we are implicitly assuming that the primordial fluctuations are purely growing modes.

Using the form of the trajectory in equation (5), we may express the derivatives of the action with respect to the coefficients as:

$$\frac{\partial S}{\partial \mathbf{C}_{i,n}} = \int dt \left[ \dot{f}_n(t) a^2 \dot{\mathbf{x}}^{(1)} + f_n \left( \nabla \phi_i^{(0)} - \nabla \phi_i \right) \right] , \quad (7)$$

where  $\phi_i^{(0)}$ , is the potential on particle,  $i$ , in the unperturbed potential field.

An integral by parts of equation (7) yields the expression:

$$\frac{\partial S}{\partial \mathbf{C}_{i,n}} = \int dt f_n \left[ -\frac{\partial(a^2 \dot{\mathbf{x}}_i^{(1)})}{\partial t} + \left( \nabla \phi_i^{(0)} - \nabla \phi_i \right) \right] = 0 . \quad (8)$$

Since the expression in the brackets is always satisfied whenever the equations of motion of the individual particles are satisfied, we may equivalently minimize:

$$X^2 = \sum_i \int dt |W(t)\mathbf{g}_i(t)|^2 \quad (9)$$

where  $W(t)$  is an arbitrary weighting function and

$$\mathbf{g}_i(t) \equiv -\frac{\partial(a^2\dot{\mathbf{x}}_i^{(1)})}{\partial t} + (\nabla\phi_i^{(0)} - \nabla\phi_i) \quad (10)$$

By finding values of the coefficients for which equation (9) vanishes, we find trajectories which satisfy the equations of motion. We then evaluate the trajectories at early times, and use the positions and velocities at high redshift as input into an ordinary N-body code. The output of the N-body code may be further used as input to a new iteration for PLA.

### 3. A Two Halo Model of an Isolated Local Group

#### 3.1. The Simulations

We now turn our attention to the simulations used to reconstruct the Local Group. Our primary goal in these simulations will be to identify the radial velocity between the two principle elements of the Local Group (the Galaxy and M31), as a function of galaxy mass and cosmology.

In order to do this, we ran two sets of simulations, one with  $\Omega_M = 0.3$ , and  $\Omega_\Lambda = 0.7$  (Cosmology 1), and the other, with  $\Omega_M = 1$  and  $\Omega_\Lambda = 0$  (Cosmology 2). In each case, we assumed  $h = 0.65$ , where the Hubble constant,  $H_0$ , is define as  $100h$  km/s/Mpc. The PLA reconstructions were run in a  $(10\text{Mpc})^3$  box, with  $64^3$  particles, and  $128^3$  gridcells, resulting in a separation of  $\sim 10$  gridcells between the centers of the two galaxies.

For each cosmology, we set up 5 different target particle fields, each based on somewhat differing assumed galaxy masses. The density profiles of the target used the form of the halo density given by Dehnen and Binney (1998):

$$\rho_h = \rho_0 \left(\frac{r}{r_0}\right)^{-\gamma} \left(1 + \frac{r}{r_0}\right)^{\gamma-\beta} \exp(-r^2/r_t^2), \quad (11)$$

where we have explicitly assumed isotropic halos, and  $\gamma$ ,  $\beta$ ,  $r_0$ ,  $\rho_0$ , and  $r_t$  are parameters of the model. We chose this parameterization over the more familiar form of Navarro, Frenk, & White (1997) because Dehnen & Binney provide fits for the Galaxy according to this form.

For each model, we hold  $\gamma = -2$ ,  $\beta = 2.959$ ,  $r_0 = 3.83$  kpc, and  $r_t = 700$  kpc fixed, and vary values of  $\rho_0$  in order to probe different combinations of galaxy masses. We find variations in mass and cosmology were clearly more important than the fine details of halo density profile. Moreover, our resolution scale was such that we treat the MW “galaxy” halo as including all of its nearby satellite galaxies.

### 3.2. Results

A summary of the results of the ten realizations are shown in Table 1. In it, we show the masses of the reconstructed galaxies within  $\bar{\delta}(r) = 200$ , their velocities along the x-axis, and the masses of the “target” galaxies within  $\bar{\delta}(r) = 200$ . Velocities are given in km/s with respect to expanding coordinate system. Since the assumed separation of the galaxies is 760 kpc, and  $h = 0.65$ , the “observed” radial velocity for each is given as:

$$u_r = v_r^{M31} - v_r^{MW} + H_0 r = v_r^{M31} - v_r^{MW} + 49 . \quad (12)$$

Overall, the quality of the reconstruction is quite good. Comparison of the observed galaxy masses to the masses measured in the target field yields agreement to about 20%. Generally, the reconstructed mass is somewhat smaller than the target mass since small errors in the computed particle trajectories result in an overall smoothing in the density field. The axial symmetry of the problem resulted in tangential velocities of typically only 1 or 2 km/s.

We now turn to an interpretation of these results. Figure 2 shows a plot of the data in Table 1, combined with the equation (12). What is quite intriguing about these mass estimates is that according to the PLA reconstruction, the two-body mass estimate of the LG *overestimates* the mass of the galaxy halos. However, one’s intuition would suggest that since the two-body estimate does not evolve from collapsed halos, the true forces should be softer than those used by Kahn & Woltjer. These means that we might expect that the two-body estimate underestimates the true mass. However, this argument may be flawed as it does not take into account the detailed collapse of the galaxies, which makes the situation much more complex. Moreover, Branchini & Carlberg (1995) suggest the same effect using N-body simulations.

We perform a similar experiment here in order to check the consistency of the mass and velocity estimates. We ran a series of N-body simulations in a flat,  $\Omega_M = 0.3$  cosmology, and extracted out all halos within a mean overdensity of  $\bar{\delta} = 200$ . We then selected those halo pairs which formed two member associated groups (i.e. those which were falling in toward one another). N-body codes all for a self-consistent scaling of the box size, velocities, and

masses of the particles. For each pair, we set the scaling factor to give a galaxy separation of 760 kpc. The resulting group masses and velocities are plotted in Figure 3 along with the masses and velocities for the reconstructed LG in the  $\Omega_M = 0.3$  reconstruction set.

It is clear from Figure 3 that the overall mass-velocity relation determined from the reconstruction is generally consistent with that generated from randomly realized N-body simulations, though the best fit slope of this relation differs by  $\sim 12\%$  (suggesting that the PLA reconstruction provides a slight mass underestimate). Moreover, it is clear that there is significantly greater scatter in the random realizations than in the reconstructed halos. This is due to the fact that the PLA reconstruction contains no outside, tidal forces, while the randomly realized field will necessarily have small halos scattered nearby.

As for the comparison of the mass-velocity relationship between the two cosmologies in the reconstruction, as illustrated in Figure 2, Cosmology 1 produces a systematically larger radial velocity for a given Local Group mass than does Cosmology 2. This accords with the relationship given by the two-body problem, and shown in Figure 1, but we may use a slightly better argument in order to estimate what this scaling ought to be.

We will address this scaling using a simple Zel’dovich model. Linear theory predicts that for small perturbations, the velocity field can be expressed as:

$$\nabla \cdot \mathbf{v}(\mathbf{x}, t) = -\frac{a\dot{D}}{\dot{a}D}\delta(\mathbf{x}, t) = -f(\Omega_M, \Omega_\Lambda, t)\delta(\mathbf{x}, t) . \quad (13)$$

However,  $f(\Omega_M, \Omega_\Lambda, t) \propto \Omega^{0.6}$ , as was pointed out by Peebles (1980, §14). In order to form a structure of a given mass,  $\delta \propto M/\Omega_M$ . Thus, we find the relation:

$$\mathbf{v} \propto \Omega_m^{-0.4} M , \quad (14)$$

where the constant of proportionality is assumed to be a function of separation and Hubble constant, both of which are kept constant in all of the simulations.

In fact, we find a somewhat shallower relation, as illustrated by the best fit lines in Figure 2. If we assume:

$$v_r = u_r + H_0 r \propto M_{tot} \Omega_M^n , \quad (15)$$

then the observed coefficient for our simulations is only  $n \simeq -0.27$ .

In Figures 4 and 5 we show some the orbits of randomly selected MW particles in Model 5 of Cosmology 1 ( $\Omega_M = 0.3$ ) in order to illustrate that even though the initial and final particle positions were constrained to provide a first collapse solution, this does not mean that the particles have not experienced orbit crossings. Figure 4 shows this explicitly, by illustrating the x-coordinate (in kpc) of 10 randomly selected MW particles. Each

particle selected was found between 100 – 200 kpc from the Galaxy center at  $z = 0$ . As expected from a typical orbital velocity of 100 – 200 km/s, they all seem to have orbited the galaxy center of mass several times by the end of the simulation. This is likewise illustrated by Figure 5, which shows a trace of the orbits as viewed from the  $z$ - and  $y$ - axes.

As another interesting test of the robustness of the reconstructions, we took one of the simulations, (# 5 in Cosmology 1), and smoothed the small scale power using a Gaussian filter with diameter 400 kpc. We then increased the resolution by a factor of two, as described in GS, multiplying the number of particles by 8, and filling in small scale power randomly using an assumed CDM power spectrum. We then ran that resulting simulation through a PM code, and recovered the LG characteristics, as shown in Model 5a in Table 1. While the total radial velocity did not change much from the low to high-resolution form of the reconstruction, and while the mass of “M31” stayed approximately constant, The Galaxy increased by  $\sim 70\%$  in mass in the high resolution case.

Though the specific details of the reconstruction differ somewhat in increasing the resolution, it is reassuring to see that the Local Group reconstruction is qualitatively similar to the low resolution case.

#### 4. Discussion

We have endeavored to reproduce the two major systems in the Local Group, the Milky Way, and M31 using the PLA approach. This was motivated by the seeming discrepancy introduced by the masses estimated by using the timing argument, and the much lower masses given by observations of the dynamics around the two halos. We have shown that by treating the galaxies as halos, rather than as point sources, and constraining the current separation and peculiar velocities to those observed, a much more consistent estimate of masses may be obtained.

As illustrated in Figure 2, though PLA can be applied to the Local Group to theoretically discriminate between a high- and low-density universe, the mass observations are currently not sufficiently tight to make such a determination practical with only two galaxies. However, it may be practical to re-address the specific program suggested by Shaya, Peebles, & Tully (1995). In that, we do not simply treat the Local Group as two objects, but rather, treat the two objects in a much larger, and interacting context.

In future work, we will reconstruct not only the major halos of the Local Group, but also add the effects of nearby groups like the Sculptor Group (Jerjen, Freeman, & Bingelli, 1998), the Centaurus A Group (van den Bergh 1999a), and the Antlia-Sextans group (van

den Bergh 2000a). Indeed, to properly treat the problem, one would prefer an external potential field out to distances well into the linear regime. While this last may be applied directly using linear theory, the nearby groups must be themselves reconstructed. This requires a larger simulation volume, but the resolution length must be maintained in order to differentiate between the Milky Way and M31. Thus, the simulation scale, (e.g., the number of particles) and thus its computation time and memory requirements, will get large with the application of even a few nearby groups, as the distance to even the nearest group, Ant-Sex, is about 3 times the radius of the Local Group, itself. A realistic reconstruction would thus require a simulation box of about three times the size of those used in the present discussion.

I would like to gratefully acknowledge many helpful comments by David Spergel, Michael Strauss, and Jim Peebles. This work was supported by an NSF Graduate Research Fellowship and NASA ATP grant NAG5-7154.

## REFERENCES

- Binney, J. & Tremaine, S. 1987, “Galactic Dynamics” (Princeton: Princeton University Press)
- Branchini, E. & Carlberg, R.E. 1995 MmSAI 66, 219
- Courteau, S. & van den Bergh, S. 1999, AJ, in press
- Dehnen, W. & Binney, J. 1998, MNRAS, 294, 429
- Dunn, A.M. & Laflamme, R. 1995 ApJ 443,1L
- Evans, N.W. & Wilkinson, M.I. 2000, submitted to MNRAS
- Goldberg, D.M. & Spergel, D.N., 2000, (GS) accepted to ApJ
- Goldberg, D.M. 2000, submitted to ApJ
- Governato, F., Moore, B., Cen, R. Stadel, J., Lake, G., & Quinn, T. 1997, NewA 2, 91
- Hockney, R.W. & Eastwood, J.W. 1981, “Computer Simulations Using Particles” (New York: McGraw Hill)
- Holland, S. 1998, AJ, 115, 1916
- Jerjen, H., Freeman, K.C., & Binggeli, B. 1998, AJ, 116, 2873
- Kahn, F.D. & Woltjer, L. 1959, ApJ, 130, 705
- Lynden-Bell, D., Cannon, R. D., & Godwin, P. J. 1983, MNRAS, 204, 87
- Mateo, M. 1998, ARA&A 36, 435
- Navarro, J.F., Frenk, C.S., & White, S.D.M. 1997, ApJ, 490, 493
- Nusser, A. & Branchini, E. 1999 astro-ph/9908167
- Peebles, P. J. E. 1980, “The Large-Scale Structure of the Universe” (Princeton: Princeton University Press)
- Peebles, P.J.E. 1989, ApJ, 344,L53
- Peebles, P.J.E. 1993, “Principles of Physical Cosmology” (Princeton: Princeton University Press)

- Peebles, P.J.E. 1994, ApJ, 429, 43
- Schmoldt, I. M. & Saha, P. 1998, AJ 115, 2231
- Shaya, E.J., Peebles, P.J.E., & Tully, R.B. 1995, ApJS 454, 15
- van den Bergh, S. 1999, A&ARv, 9 273
- van den Bergh, S. 1999a, ApJ, 517, 97
- van den Bergh, S. 2000, “The Galaxies of the Local Group” (Cambridge University Press)
- van den Bergh, S. 2000a, AJ, 119, 609
- Wilkinson, M.I. & Evans, N.W., MNRAS, 310, 645
- Zel’dovich, Y.B. 1970, A&A, 5, 84
- Zaritsky, D. 1999, in “The Galactic Halo,” Eds. Gibbon, B.K, Axelrod, T.S.,& Putman, M.E. (San Francisco: ASP)

Cosmology 1: $\Omega_M = 0.3$						
Model	$M_{MW}(\times 10^{12} M_\odot)$	$M_{M31}(\times 10^{12} M_\odot)$	$v_r^{MW}$	$v_r^{M31}$	$M_{MW}^{Target}$	$M_{M31}^{Target}$
1	1.41	0.86	69	-103	1.91	1.00
2	0.89	0.94	75	-72	1.28	1.31
3	1.02	1.10	106	-107	1.38	1.43
4	0.62	0.74	67	-65	1.14	1.18
5	0.86	0.81	75	-79	1.49	1.27
5a	1.48	0.73	48	-99	1.49	1.27
Cosmology 2: $\Omega_M = 1.0$						
	$M_{MW}(\times 10^{12} M_\odot)$	$M_{M31}(\times 10^{12} M_\odot)$	$v_r^{MW}$	$v_r^{M31}$	$M_{MW}^{Target}$	$M_{M31}^{Target}$
1	0.99	1.02	46	-49	1.02	0.87
2	1.14	1.07	73	-70	1.22	1.08
3	1.49	1.01	53	-80	1.56	1.12
4	2.09	1.56	100	-148	2.90	1.78
5	1.74	1.09	79	-110	2.25	1.53

Table 1: A summary of the results of the various Local Group reconstructions. Listed are the integrated masses out to an overdensity of  $\delta = 200$ , in units of  $10^{12} M_\odot$ , the mean velocity along the x-axis of the particles within each galaxy in units of km/s, and the actual mass of the galaxies used in the target density field. Note that to get the observed radial velocity, one needs to compute  $u_r = v_{M31} - v_{MW} + H_0 r$ , where the last term is approximately 49 km/s for  $h = 0.65$  and  $r = 760 kpc$ .

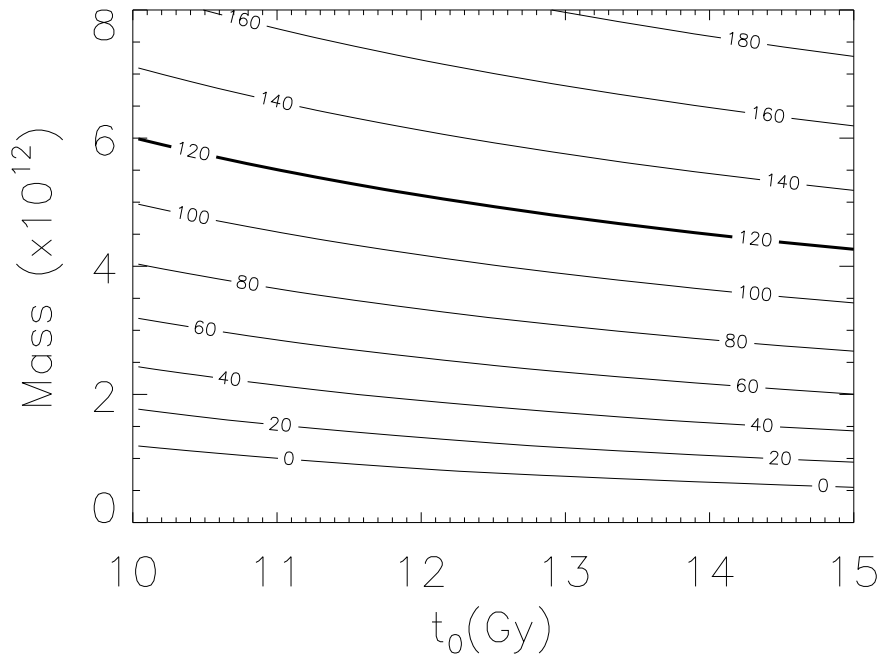


Fig. 1.— The relationship between imputed Local Group mass, the age of the universe, and predicted radial velocity (shown in the contour plot) according to the two-body approximation. Note that under no assumed age does the corresponding predicted mass match observations.

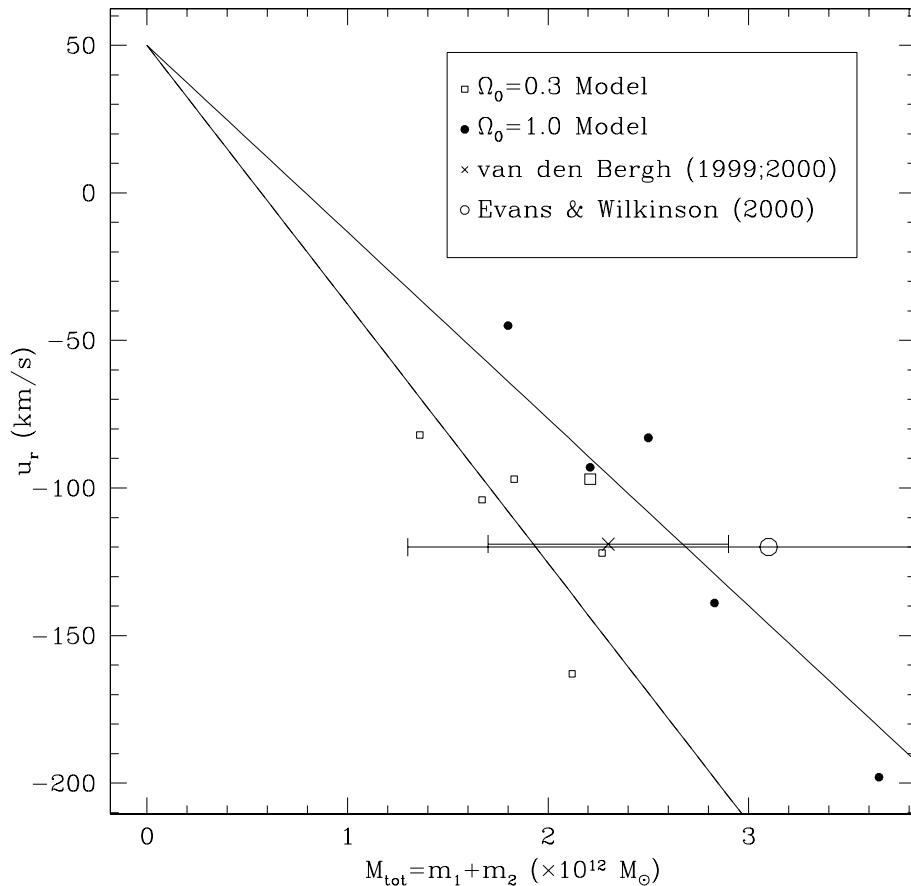


Fig. 2.— The relationship between total Local Group mass and “observed” radial velocities for the reconstructed LG models under  $\Omega_M = 0.3$  and  $\Omega_M = 1.0$  cosmologies, with a comparison to actual mass estimates of the Local Group. The open squares indicate Cosmology 1 ( $\Omega_M = 0.3$ ), while the larger square shows the results of the high-resolution realization. The filled circles represent Cosmology 2 ( $\Omega_M = 1.0$ ). Note that given the error bars in the observed masses of M31 and the Milky way, strong constraints cannot yet be made on cosmology from these models.

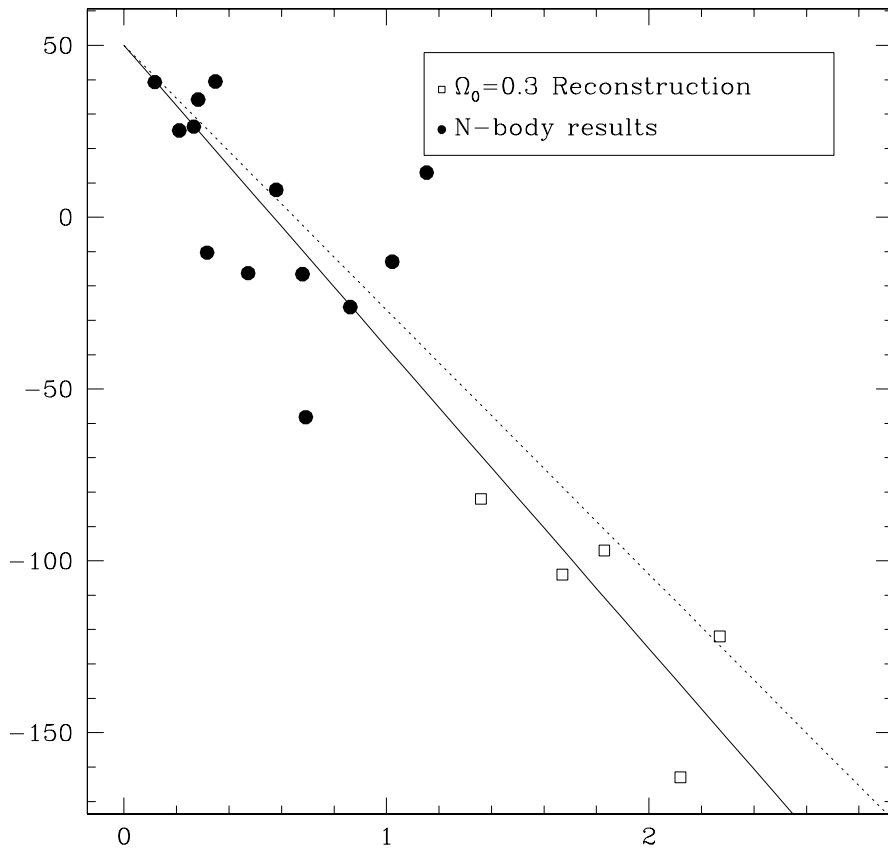


Fig. 3.— As in the previous figure, the relationship between total Local Group mass and “observed” radial velocities for the reconstructed LG models under the  $\Omega_M = 0.3$  PLA reconstruction, and a randomly realized set of Local Groups found in an N-body simulation. The open squares indicate the PLA reconstruction, and the filled circles show the simulation. The solid line represents the best fit mass-velocity relation for PLA, while the dashed line represents a similar fit for the simulations.

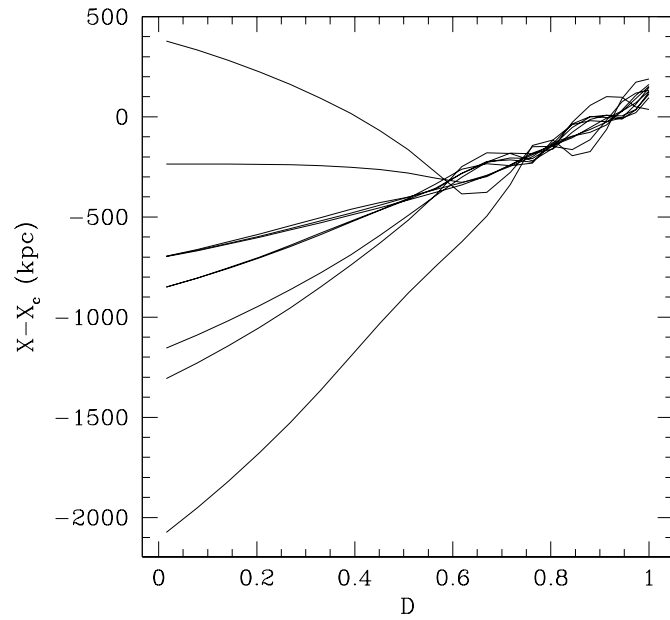


Fig. 4.— X-coordinate orbits of 10 randomly selected MW particles in Simulation 5 of Cosmology 1 ( $\Omega_M = 0.3$ ). Each particle was selected from 100 – 200 kpc of the MW center. Note that there are typically several orbit crossings over the course of the realization.

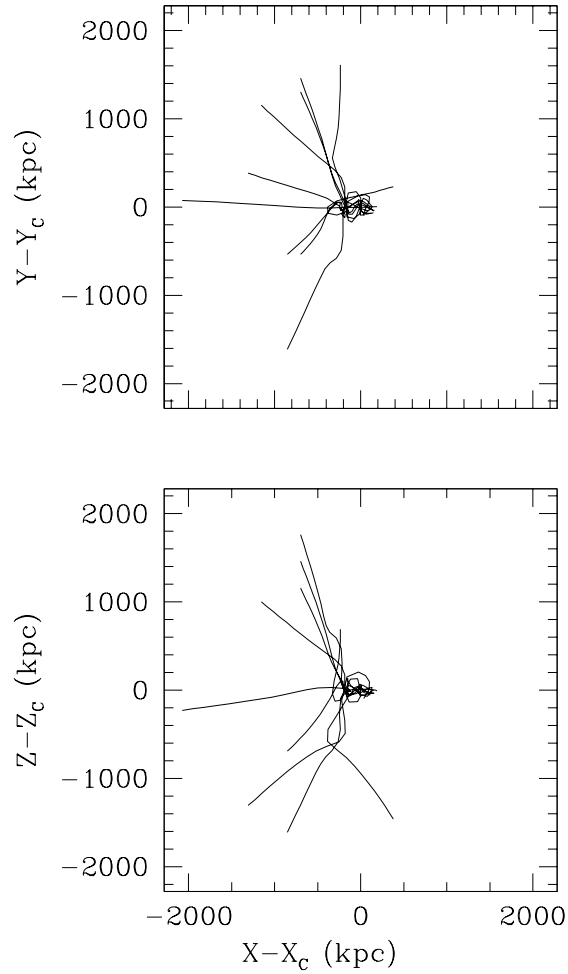


Fig. 5.— A trace of 10 orbits randomly selected MW particles in Simulation 5 of Cosmology 1 ( $\Omega_M = 0.3$ ). The top panel shows the orbits in the X-Z plane, while the bottom panel shows the orbits in the X-Y plane.